

# Effect of ZrO<sub>2</sub> on Radiation Shielding Properties of xZrO<sub>2</sub>-(55-x) B<sub>2</sub>O<sub>3</sub>-15Bi<sub>2</sub>O<sub>3</sub>-10MgO-20PbO Glass: XCOM and Phy-X/PSD Database Software

Oki Ade Putra<sup>1</sup>, Suci Faniandari<sup>1</sup>, Dhani Nur Indra Syamputra<sup>1</sup>,  
Muhammad Fahmi<sup>1</sup>, Erik Bhekti Yutomo<sup>1</sup>

<sup>1</sup>Department of Physics, Faculty of Science and Mathematic, Diponegoro Univeristy, Semarang, Indonesia

Corresponding Author: Oki Ade Putra

DOI: <https://doi.org/10.52403/ijrr.20241110>

## ABSTRACT

This paper aims to determine the effect of ZrO<sub>2</sub> on the parameters of glass-based radiation shielding with the molecular formula xZrO<sub>2</sub>-(55-x)B<sub>2</sub>O<sub>3</sub>-15Bi<sub>2</sub>O<sub>3</sub>-10MgO-20PbO (mole fraction, x= 0, 4, 8, 12, and 16 mol%). The parameters tested include Mass Attenuation Coefficients (MAC), Linear Attenuation Coefficient (LAC), Half-Value Layer (HVL), Tenth-Value Layer (TVL), Mean Free Path (MFP), and Effective Atomic Number (Z<sub>eff</sub>), which are measured using the XCOM and Phy-X/PSD programs in the energy range between 0.015 MeV and 15 MeV. The MAC values obtained for all samples are between 0.0439-76.4100 cm<sup>2</sup>/g for 0ZrO, 0.0440-75.9300 cm<sup>2</sup>/g for 4ZrO, 0.0441-75.4700 cm<sup>2</sup>/g for 8ZrO, 0.0443-75.0200 cm<sup>2</sup>/g for 12ZrO, 0.0444-74.5800 cm<sup>2</sup>/g for 16ZrO. The difference in results between XCOM and Phy-X/PSD is very small, less than 0.1%. Compared with commercial shields such as RS-253-G18 glass shield and 40% synthetic borax radiation shield, ZrO<sub>2</sub>-based glass shield has better radiation capability. The 16ZrO sample has the best quality among all ZrO<sub>2</sub>-based glass shield samples at various radiation photon energies. This study is expected to be a reference in making glass radiation shields in further experiments.

**Keywords:** Radiation Shielding, Zirconium Oxide, Bi<sub>2</sub>O<sub>3</sub>, XCOM, Phy-X/PSD, S

## INTRODUCTION

The increasingly widespread use of ionizing radiation needs to be balanced with increased safety standards to protect workers from the side effects that can be caused by radiation. Three main strategies to reduce the effects of radiation are reducing exposure time, increasing distance from the radiation source, and using radiation shields (1). Researchers focus on developing effective, environmentally friendly radiation shielding materials that can be used in various systems to produce the best shield.

There are several types of radiation shielding materials, including concrete. Concrete-based radiation shields have many weaknesses, such as their rigid shape, so they cannot be used in portable radiation systems or rooms with limited space. In addition, concrete requires a large thickness and the use of lead in large concentrations, which is harmful to the environment and human health because it is toxic (2). One alternative shielding material is glass because it has several advantages over concrete. Glass is transparent, so radiation workers can still see from behind the shield while protecting it from radiation. The manufacturing process is relatively more straightforward and can be combined with other types of materials to improve the quality of the shield. In addition,

Glass has more flexible accessibility because it can be shaped according to needs, including portable radiation systems. Another advantage of Glass is its high-temperature resistance, which is better than polymer-based shields (3).

Several researchers have researched the basic materials for glass shield systems. As reported in the study (4) evaluated the effect of ZnO on the B<sub>2</sub>O<sub>3</sub>-PbO-ZnO-CaO glass system. The results showed that adding ZnO improved the radiation shielding quality, with a Linear Attenuation Coefficient (LAC) value of 11.136 cm<sup>-1</sup> at an energy of 0.060 MeV. Another study on the effect of CdO metal oxide on the CoO-Na<sub>2</sub>O-B<sub>2</sub>O<sub>3</sub> glass system conducted by (5) resulted in the Half Value Layer (HVL) value being 4.421 cm at an energy of 1.333 MeV. This study shows that the higher the concentration of CdO, the better the quality of the radiation shield produced. However, both of these studies are still limited in using relatively low radiation energy, namely maximum radiation at an energy of 1.33 MeV. Another study by (6) looked for the effect of TiO<sub>2</sub> on the La<sub>2</sub>O<sub>3</sub>-B<sub>2</sub>O<sub>3</sub>-Gd<sub>2</sub>O<sub>3</sub>-Nb<sub>2</sub>O<sub>5</sub>-ZrO<sub>2</sub>-SiO<sub>2</sub> glass system. The addition of TiO<sub>2</sub> improved the performance of the radiation shield, with the Mass Attenuation Coefficient (MAC) value at an energy level of 0.15 MeV being 0.5271 cm<sup>2</sup>/g. However, like previous studies, the radiation energy used in this study was also still low, namely 0.15 MeV. So, other research is needed to use higher energy levels.

Zirconia (ZrO<sub>2</sub>) is one of the potential radiation shielding materials for use in glass-based systems. This is because it has a relatively high atomic number (40) and mass number (91.22), contributing to its ability to absorb high-energy radiation, such as X-rays and gamma rays. With its high density, ZrO<sub>2</sub> can block radiation more effectively than other materials with lower atomic numbers (7). In addition, this material has excellent thermal and chemical stability, making it resistant to degradation, even in environmental conditions with high radiation intensity. Another advantage of ZrO<sub>2</sub> is its

ability to maintain transparency in glass compositions and good mechanical strength. This allows the material to be used in radiation shielding applications without sacrificing visibility and resistance to physical impact (8).

This study aims to determine the performance of glass shields containing ZrO<sub>2</sub> metal oxide in the xZrO<sub>2</sub>-(55-x)B<sub>2</sub>O<sub>3</sub>-15Bi<sub>2</sub>O<sub>3</sub>-10MgO-20PbO shield system, where x represents mol% ZrO<sub>2</sub> with variations of 0, 4, 8, 12, and 16. The main parameters that determine the quality of the radiation shield are evaluated to validate the working ability of the glass shield and the effect of adding ZrO<sub>2</sub> on the performance of the quality of the glass-based radiation shield. Several parameters tested, such as Mass Attenuation Coefficient (MAC), Linear Attenuation Coefficient (LAC), Half-Value Layer (HVL), Tenth-Value Layer (TVL), Mean Free Path (MFP), and adequate atomic number ( $Z_{\text{eff}}$ ), in the energy range of 0.015 to 15 MeV. These values are obtained from simulations using the XCOM and Phy-X/PSD programs. The results of the processed data are compared with several other commercial shields, such as glass and concrete shields. So, it is hoped that this research will be a reference material for making ZrO<sub>2</sub>-based glass shields in the experimental process.

## **METHODS**

In this study, variations of ZrO<sub>2</sub> material were carried out on glass-based radiation shields with the chemical formula xZrO<sub>2</sub>-(55-x)B<sub>2</sub>O<sub>3</sub>-15Bi<sub>2</sub>O<sub>3</sub>-10MgO-20PbO. The radiation shielding ability was measured using the XCOM program and Phy-X/PSD, and then several supporting parameters were sought, such as Mass Attenuation Coefficients (MAC), Linear Attenuation Coefficient (LAC), Half-Value Layer (HVL), Tenth-Value Layer (TVL), Mean Free Path (MFP) and Effective Atomic Number ( $Z_{\text{eff}}$ ). The atomic number and mass number of each component of the shielding glass material are shown in Table 1.

**Table 1 : Atomic and mass number of each element that makes up the protective glass (R. Lide, 2004)**

Element	Atomic Number (Z)	Atomic Mass (A)
B	5	10.0129
O	8	15.9949
Mg	12	23.9850
Zr	40	89.9047
Pb	82	203.9730
Bi	83	208.9803

The test was conducted on five samples based on the variation of mol% ZrO<sub>2</sub> concentration. Each sample will be analyzed at 12 levels of radiation energy. Table 2 describes the variation of each sample's

composition, the mole fraction (mol%) of each component, and its density. The general molecular formula is xZrO<sub>2</sub>-(55-x)B<sub>2</sub>O<sub>3</sub>-15Bi<sub>2</sub>O<sub>3</sub>-10MgO-20PbO.

**Table 2: Fraction of the Component (mol.%) and density of each sample**

Sample	ZrO <sub>2</sub>	B <sub>2</sub> O <sub>3</sub>	Bi <sub>2</sub> O <sub>3</sub>	MgO	PbO	Density (g/cm <sup>3</sup> )
0ZrO	0	55	15	10	20	3.552
4ZrO	4	51	15	10	20	3.665
8ZrO	8	47	15	10	20	3.785
12ZrO	12	43	15	10	20	3.913
16ZrO	16	29	15	10	20	4.050

Based on Table 2 shows an increasing trend in the density of the mixture as the chemical composition of ZrO<sub>2</sub> increases, with the highest value at 16ZrO (16 mol% ZrO<sub>2</sub>) with

a density value of 4,050 g/cm<sup>3</sup>. Meanwhile, table 3 explains the variation of each component and the weight fraction (wt%) of each constituent element.

**Table 3: Fraction of the element (wt.%) of each sample**

Sample	Zr	O	B	Bi	Mg	Pb
0ZrO	0	0.2448	0.0758	0.3996	0.0154	0.2641
4ZrO	0.0229	0.2374	0.0693	0.3943	0.0152	0.2606
8ZrO	0.0452	0.2303	0.0630	0.3890	0.0150	0.2571
12ZrO	0.0670	0.2234	0.0569	0.3839	0.0148	0.2537
16ZrO	0.0882	0.2166	0.0509	0.3789	0.0146	0.2504

The calculation of MAC parameters was carried out using the XCOM program developed by the NIST (National Institute of Standards and Technology) database. This program is used to calculate scattering, photoelectric absorption, and pair production at photon energies in the range from 0.001

MeV to 20 MeV theoretically (9). In addition, Phy-X/PSD software was used to calculate radiation shielding and dosimetry parameters (10). Both programs are used as the basis for calculating radiation shielding parameters, which are then compared.

**Table 4: Chemical composition of glass shielding samples**

Sampel Code	Sample, x	xZrO <sub>2</sub> -(55-x)B <sub>2</sub> O <sub>3</sub> -15Bi <sub>2</sub> O <sub>3</sub> -10MgO-20PbO	Density (g/cm <sup>3</sup> )
0ZrO	0	0ZrO <sub>2</sub> -55B <sub>2</sub> O <sub>3</sub> -15Bi <sub>2</sub> O <sub>3</sub> -10MgO-20PbO	3.552
4ZrO	4	4ZrO <sub>2</sub> -(51)B <sub>2</sub> O <sub>3</sub> -15Bi <sub>2</sub> O <sub>3</sub> -10MgO-20PbO	3.665
8ZrO	8	8ZrO <sub>2</sub> -(47)B <sub>2</sub> O <sub>3</sub> -15Bi <sub>2</sub> O <sub>3</sub> -10MgO-20PbO	3.785
12ZrO	12	12ZrO <sub>2</sub> -(43)B <sub>2</sub> O <sub>3</sub> -15Bi <sub>2</sub> O <sub>3</sub> -10MgO-20PbO	3.913
16ZrO	16	16ZrO <sub>2</sub> -(39)B <sub>2</sub> O <sub>3</sub> -15Bi <sub>2</sub> O <sub>3</sub> -10MgO-20PbO	4.050

LAC is a parameter used to measure the rate of reduction in the intensity of ionizing radiation when passing through a particular material. This value directly correlates to the material's ability to absorb or retain radiation (11). The greater the LAC value, the better the material's ability to shield radiation. To calculate the LAC value, it can be done by calculating using the Lambert-Beer equation (6) with the equation as below:

$$I = I_0 e^{-\mu x} \quad (1)$$

Where, I<sub>0</sub> is the radiation intensity before passing through the shielding material, and I is the intensity after passing through the shielding material. μ is LAC (cm<sup>-1</sup>), and x is the thickness of the radiation shielding material (cm).

MAC is a parameter that indicates how much a material absorbs radiation per unit density (11). Unlike LAC, which measures absorption per unit length, MAC considers the density of the material, thus providing a more universal picture of the absorption capacity of a material. MAC can be used to compare the quality of the absorption capacity between shielding materials. The greater the MAC value, the better the quality of the shielding material produced. The equation for calculating MAC is divided by the LAC value and the density of the constituent materials. The composite MAC value depends on (μ/ρ)<sub>i</sub> and the mass fraction (w<sub>i</sub>) of each component of the glass-based shielding material (12).

$$MAC = \frac{\mu}{\rho} = \sum_i w_i \left( \frac{\mu}{\rho} \right)_i \quad (2)$$

Other parameters affecting shielding glass performance quality are HVL and TVL, which have similar concepts. Based on its definition, HVL is the ability of a shielding material to reduce the intensity of ionizing radiation by half, while TVL is to reduce the intensity of radiation by one-tenth (13). The equations of HVL and TVL are derived from the MAC value:

$$HVL (cm) = \frac{\ln 2}{\mu (cm^{-1})} \quad (3)$$

$$TVL (cm) = \frac{\ln 10}{\mu} \quad (4)$$

MFP is the average distance radiation particles travel before interacting with atoms in the shielding material, which causes a reduction in radiation energy. The shorter the MFP of a material, the more influential the material is in blocking or reducing radiation exposure. The MFP value can be determined by the following equation (14):

$$MFP (cm) = \frac{1}{\mu (cm^{-1})} \quad (5)$$

Z<sub>eff</sub> is the adequate atomic number of a material used as a radiation shield (15). Z<sub>eff</sub> is an important parameter that describes the ability of a material to absorb or inhibit ionizing radiation. The higher the Z<sub>eff</sub> value of a material, the more influential it is in absorbing radiation because it has more electrons that can interact with photon radiation. These interactions include the photoelectric effect, Compton scattering, or pair production. The equation for calculating Z<sub>eff</sub> can be found by calculating the ratio between the total atomic cross-section (σ<sub>a</sub>) and the total electronic cross-section (σ<sub>e</sub>) (6) (10):

$$Z_{eff} = \frac{\sigma_a}{\sigma_e} = \frac{\sum_i f_i A_i \left( \frac{\mu}{\rho} \right)_i}{\sum_i f_i Z_j^A \left( \frac{\mu}{\rho} \right)_j} \quad (6)$$

f<sub>i</sub>, A, and Z are the molar fractions, atomic mass per mole, and atomic number of the i<sup>th</sup> element in the component, respectively.

## RESULT AND DISCUSSION

The higher the MAC value of a shielding material, the better the quality of the material in absorbing radiation. Two factors affect the MAC value, namely energy and material density. Generally, the greater the intensity of radiation energy, the lower the MAC value (11). Based on Figure 1, the decrease in the

MAC value in the same sample and the increase in radiation energy can be seen. For example, in the 0ZrO sample, the initial

MAC value is 76.4100 cm<sup>2</sup>/g at an energy of 0.03 MeV to 0.0439 cm<sup>2</sup>/g at an energy of 15 MeV.

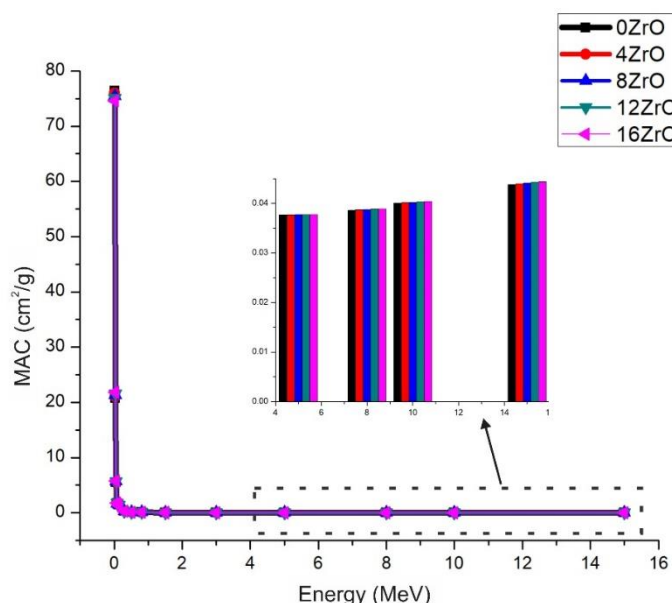


Figure 1: Mass attenuation coefficient (MAC) versus photon energy

Changes in the type of interaction between radiation and materials at various energy levels cause a decrease in MAC value. At low energy levels, the dominant interaction is the photoelectric effect, which can absorb radiation as part of the shielding system. Based on its probability, the cross-section for the photoelectric effect is inversely proportional to energy according to the formula ( $\sigma_{PE} \propto 1/E$ ) (16). At medium energy levels, the occurrence of the photoelectric effect begins to be replaced by Compton scattering (CS), where the probability of the cross-section is influenced by the value of the adequate atomic number ( $Z_{eff}$ ) with the formula ( $\sigma_{CS} \propto Z_{eff}$ ) (17). At high energy, the dominant interaction of radiation with matter is pair production (18). The decrease

in MAC value occurs in all glass shielding materials with relatively similar MAC values in each sample.

The second factor that affects the MAC value is the density of the material. The higher the density of the shielding material, the denser the electron composition of the material, thereby increasing the potential for interaction between radiation photons and electrons (12). Based on the data obtained, it can be seen that the 16ZrO sample has the highest density value compared to other samples. For example, at a radiation energy of 0.05 MeV, the MAC values are respectively 5.5430 cm<sup>2</sup>/g, 5.6080 cm<sup>2</sup>/g, 5.6720 cm<sup>2</sup>/g, 5.7340 cm<sup>2</sup>/g and 5.7940 cm<sup>2</sup>/g in samples 0ZrO, 4ZrO, 8ZrO, 12ZrO and 16ZrO.

Table 5. Comparison of Mass Attenuation Coefficient (MAC) values from XCOM and Phy-X/PSD programs

Energy (MeV)	0ZrO			4ZrO			8ZrO			12ZrO			16ZrO		
	XCOM	Phy-X/PSD	$\Delta$ (%)	XCOM	Phy-X/PSD	$\Delta$ (%)	XCOM	Phy-X/PSD	$\Delta$ (%)	XCOM	Phy-X/PSD	$\Delta$ (%)	XCOM	Phy-X/PSD	$\Delta$ (%)
0.015	76.4100	76.4100	0.0000	5.9300	75.9347	0.0006	5.4700	75.4720	0.0003	75.0200	75.0215	0.0002	74.5800	74.5826	0.0004
0.03	20.7300	20.7288	0.0006	1.0200	21.0170	0.0014	1.3000	21.2975	0.0012	21.5700	21.5706	0.0003	21.8400	21.8367	0.0015

0.05	5.5430	5.543 2	0.00 3	5.6080	5.608 4	0.0 06	5.6720	5.671 8	0.0 04	5.7340	5.733 6	0.0 08	5.794 0	5.793 7	0.0 05
0.08	1.7020	1.702 4	0.02 3	1.7170	1.717 5	0.0 27	1.7320	1.732 1	0.0 07	1.7460	1.746 4	0.0 23	1.760 0	1.760 3	0.0 17
0.15	1.4090	1.409 4	0.03 2	1.3980	1.397 9	0.0 06	1.3870	1.386 7	0.0 23	1.3760	1.375 8	0.0 18	1.365 0	1.365 1	0.0 08
0.3	0.3083	0.308 3	0.00 5	0.3062	0.306 2	0.0 05	0.3041	0.304 1	0.0 13	0.3022	0.302 1	0.0 17	0.300 2	0.300 2	0.0 04
0.5	0.1376	0.137 6	0.02 2	0.1370	0.137 0	0.0 15	0.1363	0.136 3	0.0 34	0.1357	0.135 7	0.0 21	0.135 1	0.135 1	0.0 21
0.8	0.0830	0.083 0	0.00 3	0.0827	0.082 7	0.0 01	0.0825	0.082 5	0.0 06	0.0822	0.082 2	0.0 05	0.082 0	0.082 0	0.0 04
1.5	0.0520	0.052 0	0.00 5	0.0520	0.052 0	0.0 00	0.0519	0.051 9	0.0 00	0.0518	0.051 8	0.0 04	0.051 7	0.051 7	0.0 06
3	0.0402	0.040 1	0.01 1	0.0401	0.040 1	0.0 07	0.0401	0.040 1	0.0 01	0.0401	0.040 1	0.0 06	0.040 0	0.040 0	0.0 09
5	0.0377	0.037 7	0.00 8	0.0377	0.037 7	0.0 13	0.0377	0.037 7	0.0 09	0.0377	0.037 7	0.0 06	0.037 8	0.037 7	0.0 05
8	0.0386	0.038 6	0.00 2	0.0387	0.038 7	0.0 07	0.0388	0.038 8	0.0 07	0.0388	0.038 8	0.0 02	0.038 9	0.038 9	0.0 07
10	0.0400	0.040 0	0.01 2	0.0401	0.040 1	0.0 03	0.0402	0.040 2	0.0 12	0.0403	0.040 3	0.0 10	0.040 4	0.040 4	0.0 12
15	0.0439	0.043 8	0.00 1	0.0440	0.044 0	0.0 08	0.0441	0.044 1	0.0 00	0.0443	0.044 2	0.0 01	0.044 4	0.044 4	0.0 09

In Table 4, the MAC values obtained from the XCOM and Phy-X/PSD programs have minimal differences, with the percentage difference between the two being less than 0.1%, indicating a high accuracy level in data processing because the two programs validate it. The MAC value obtained from theoretical calculations using the XCOM program is used to calculate the LAC value using equation (2). The LAC results obtained have the same trend as the MAC value; the higher the radiation energy level, the lower the LAC value produced (4). In the 4ZrO sample, the initial LAC value was 278.2835 cm<sup>-1</sup> to 0.1612 cm<sup>-1</sup> at energies of 0.0015 MeV and 15 MeV, respectively.

The LAC value is not affected by the density of the shielding material but by the increase in the mole fraction of the ZrO<sub>2</sub> compound. At the energy level of 0.15 MeV, the LAC values are 5.0048 cm<sup>-1</sup>, 5.1237 cm<sup>-1</sup>, 5.2498 cm<sup>-1</sup>, 5.3843 cm<sup>-1</sup>, and 5.5283 cm<sup>-1</sup> in

samples with 0ZrO, 4ZrO, 8ZrO, 12ZrO, and 16ZrO, respectively.

The HVL value indicates the thickness of the radiation shield required to reduce the intensity of ionizing radiation by half. The smaller the HVL value of a material, the better its performance (5). The HVL value is influenced by two main factors: the energy of the radiation photons and the density of the radiation shielding material.

The first factor is radiation energy. The higher the radiation energy, the thicker the material is required, resulting in a more considerable HVL value. In the 8ZrO sample, the HVL value increases with increasing radiation energy. At energies of 0.03 MeV, 0.8 MeV, and 15 MeV, the HVL values are 0.0086 cm, 2.2208 cm, and 4.1507 cm, respectively. These data can be explained that a thicker shield is needed to reduce the radiation intensity to half as the radiation energy increases.

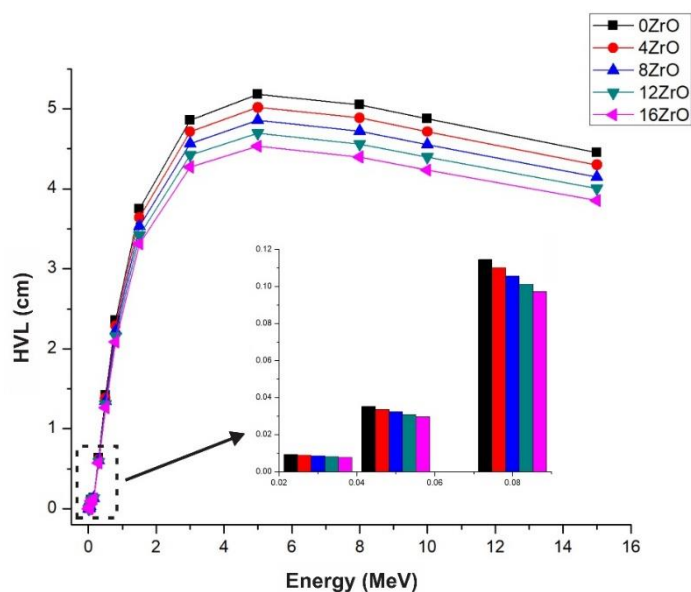


Figure 2. Half-Value Layer (HVL) value based on radiation energy

The second factor is the density of the radiation shielding material. The denser the shielding material, the higher the probability of radiation photon interaction with electrons in the material, and the smaller the HVL value (16). Based on the data obtained, at an energy level of 0.3 MeV, the HVL values of all samples were 0.6330 cm, 0.6177 cm, 0.6022 cm, 0.5862 cm, and 0.5701 cm for samples 0ZrO, 4ZrO, 8ZrO, 12ZrO, and 16ZrO, respectively. This shows that the increase in density due to adding ZrO<sub>2</sub> positively impacts reducing the HVL value of radiation shielding. Zr metal with atomic number  $Z = 40$  plays a vital role in increasing the radiation shielding ability. On the other hand, as the mole fraction of ZrO<sub>2</sub> increases, the mole fraction of Bi<sub>2</sub>O<sub>3</sub> decreases.

Another parameter similar to HVL is TVL. TVL measures the ability of natural radiation shielding materials to reduce radiation intensity by one-tenth (19). TVL has the same tendency as HVL: the TVL value will increase with the increase in the amount of incoming radiation, and at the same radiation level, the TVL value will decrease with the increase in the density and concentration of ZrO<sub>2</sub> in the shield material.

To explain the MFP value, a comparison was made with other materials, such as a commercial glass shield RS-253-G18 (20) and a 40% synthetic borax radiation shield

(21). The test was carried out at two photon energies, 0.662 MeV and 1.332 MeV, to determine the effect of ZrO<sub>2</sub> concentration on the performance of glass-based radiation shields. At an energy of 0.662 MeV, the MFP value decreases as the ZrO<sub>2</sub> content in the glass shield increases. Compared with ZrO<sub>2</sub>-based samples, the 0ZrO sample (without ZrO<sub>2</sub>) has the highest MFP value. However, compared with other types of shields, such as commercial glass shield RS-253-G18 and 40% synthetic borax radiation shield, all ZrO<sub>2</sub>-based samples have lower MFP values. The MFP values are respectively 2.8272 cm, 2.7500 cm, 2.6722 cm, 2.5940 cm, 2.5147 cm, 4.8000 cm, and 5.5000 cm for all samples of 0ZrO, 4ZrO, 8ZrO, 12ZrO, 16ZrO, RS-253-G18, and 40% synthetic borax. The smaller the MFP value, the better the quality of the radiation shield (14).

Based on the simulation results, all samples' glass shields were better than commercial shields. In addition, glass's transparent and flexible nature makes it more desirable for more comprehensive applications than other types of shields.

At an energy of 1.332 MeV, the results are the same as the radiation energy level of 0.662 MeV. The MFP value of the 16ZrO sample is 4.4601 cm lower than that of other glass samples, namely 0ZrO, 4ZrO, 8ZrO, and 12ZrO, which have values of 5.0472 cm,

4.9012 cm, 4.7544 cm, and 4.6080 cm, respectively. Even compared to commercial glass shields such as RS-253-G18 and 40% Borax radiation shields, the MFP values of the ZrO<sub>2</sub> glass shield are lower at 7.800 and

8.200, respectively. The main factor that causes this is the presence of ZrO<sub>2</sub>, which increases the radiation shielding capability by increasing the density and interaction of radiation with the shielding material.

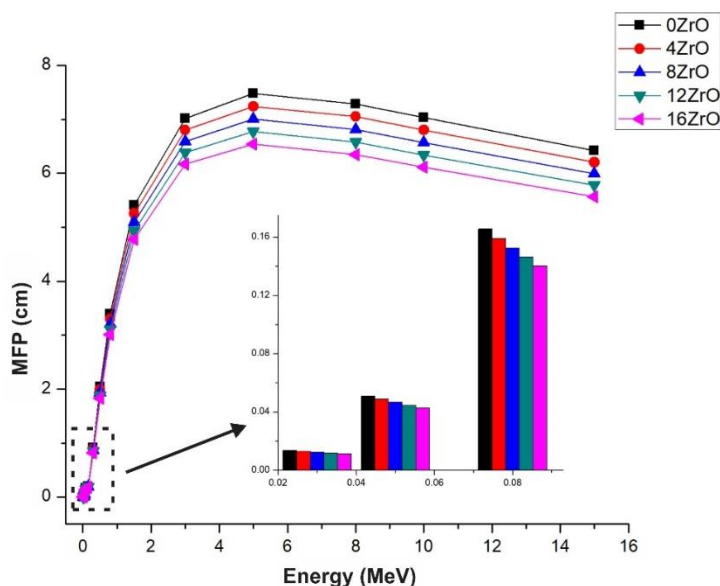


Figure 3. Mean free path (MFP) based on photon radiation energy

Compared to the same sample, such as the 12ZrO sample, the MFP value increases with incoming radiation. At energies of 0.015 MeV and 5 MeV, the MFP value increases from 0.0034 cm to 5.7753 cm, respectively. This increase in the MFP value indicates a decrease in the radiation shielding ability because the radiation photons require a longer average distance to interact with the electrons in the radiation shielding material. One of the mechanisms for reducing ionizing radiation energy by shielding materials is to increase the probability of interaction between radiation photons and electrons in the shielding material. The  $Z_{\text{eff}}$  value is a parameter that describes the electrons in the shielding material that contribute to radiation absorption. The higher the  $Z_{\text{eff}}$  value, the more influential the shield is in protecting

against radiation (5). The amount of incoming radiation energy influences the  $Z_{\text{eff}}$  value.  $Z_{\text{eff}}$  decreases in the low energy region (0.015–0.15 MeV) due to the Photoelectric Effect (PE) interaction. After 0.1 MeV, the Compton Scattering (CS) interaction becomes dominant, and  $Z_{\text{eff}}$  is inversely proportional to the energy of the radiation photons (17).

In the same sample, the  $Z_{\text{eff}}$  value decreases with increasing radiation energy. The 16ZrO sample at energies of 0.015 MeV and 1.5 MeV changed from 75.5626 to 36.8797. Adding ZrO<sub>2</sub> content at the same energy level increases the  $Z_{\text{eff}}$  value. At an energy of 1.5 MeV, the  $Z_{\text{eff}}$  values for the 0ZrO, 4ZrO, 8ZrO, 12ZrO, and 16ZrO samples are 18.5712, 19.1465, 19.7440, 20.3650, and 21.0108, respectively.



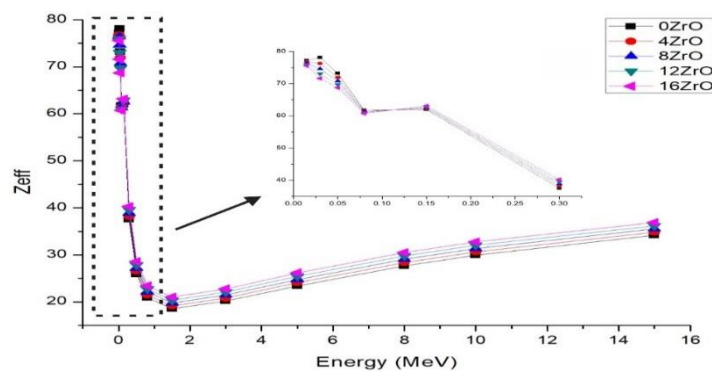


Figure 4.  $Z_{\text{eff}}$  versus based on photon radiation energy

At higher energy levels,  $Z_{\text{eff}}$  values increase after 1.5 MeV, which is caused by the occurrence of Pair Production (PP) interactions. Increasing the ZrO<sub>2</sub> content in the shielding material also increases  $Z_{\text{eff}}$  values, strengthening the radiation shielding capabilities in protecting against ionizing radiation.

## CONCLUSION

The addition of ZrO<sub>2</sub> to the glass shield with the molecular formula xZrO<sub>2</sub>-(55-x)B<sub>2</sub>O<sub>3</sub>-15Bi<sub>2</sub>O<sub>3</sub>-10MgO-20PbO (mole fraction, x = 0, 4, 8, 12, and 16 mol%) significantly affects the radiation shielding parameters such as Mass Attenuation Coefficients (MAC), Linear Attenuation Coefficient (LAC), Half-Value Layer (HVL), Tenth-Value Layer (TVL), Mean Free Path (MFP) and Effective Atomic Number ( $Z_{\text{eff}}$ ). Increasing the ZrO<sub>2</sub> content has been proven effective in increasing the shield's ability to absorb radiation. With a high atomic number ( $Z = 40$ ), ZrO<sub>2</sub> can increase the density of the material, thereby increasing the probability of interaction between radiation and the shielding material. The higher the concentration of ZrO<sub>2</sub>, the lower the HVL, TVL, and MFP values, which means that the shield thickness needed to reduce radiation is smaller. The high  $Z_{\text{eff}}$  value indicates that ZrO<sub>2</sub>-based glass shielding is more effective in absorbing radiation than commercial glass such as RS-253-G18 and 40% synthetic borax. ZrO<sub>2</sub>-based glass shielding is proven more effective in reducing radiation at various energy levels. In addition, Glass's

transparent and flexible characteristics make it more suitable for various applications than other shielding materials.

## Declaration by Authors

**Acknowledgement:** None

**Source of Funding:** None

**Conflict of Interest:** The authors declare no conflict of interest.

## REFERENCES

1. Onaizi AM, Amran M, Tang W, Betoush N, Alhassan M, Rashid RSM, dkk. Radiation-shielding concrete: A review of materials, performance, and the impact of radiation on concrete properties. *J Build Eng*. November 2024; 97:110800.
2. Hannachi E, Sayyed MI, Slimani Y, Mahmoud KA. Assessment of shielding efficiency of highly energetic electromagnetic radiation for lead-free cuprate-class material: Effect of MnFe<sub>2</sub>O<sub>4</sub> ratios. *Inorg Chem Commun*. November 2024; 169:112996.
3. Alzahrani JS, Alrowaili ZA, Sriwunkum C, Al-Buriahi MS. Radiation and nuclear shielding performance of tellurite glass system containing Li<sub>2</sub>O and MoO<sub>3</sub>: XCOM and FLUKA Monte Carlo. *J Radiat Res Appl Sci*. Juni 2024; 17(2):100923.
4. Almuqrin AH, Sayyed MI, Khandaker MU, Elsafi M. Exploring the impact of Bi<sub>2</sub>O<sub>3</sub> particle size on the efficacy of dimethylpolysiloxane for medical gamma/X-rays shielding applications. *Radiat Phys Chem*. Juli 2024; 220:111629.
5. Maatouk A, Almotawa RM, Alshehri SA, Sayyed MI, Qutub MAZ, Amin HY, dkk. Compositional impacts of high CdO content on the structure and radiation shielding efficiency of CoO-Na<sub>2</sub>O-B<sub>2</sub>O<sub>3</sub> glass

- system. Radiat Phys Chem. Desember 2024; 225:112142.
6. Hoşgör G, Tabar E, Kemah E, Yakut H. Influence of TiO<sub>2</sub> content on the radiation shielding properties of the La<sub>2</sub>O<sub>3</sub>-B<sub>2</sub>O<sub>3</sub>-Gd<sub>2</sub>O<sub>3</sub>-Nb<sub>2</sub>O<sub>5</sub>-ZrO<sub>2</sub>-SiO<sub>2</sub> glasses. Radiat Phys Chem. Januari 2025; 226:112281.
  7. El-Khayatt AM, Alghamdi AA, Sabik A, Altoub T, Saudi HA. Effect of ZrO<sub>2</sub> on physical and radiation shielding properties of tellurium -lead- calcium -borate (TPCB)glass system. Ann Nucl Energy. September 2024; 205:110576.
  8. Alrowaili ZA, Yılmaz E, Çalışkan F, Öztürk B, Olarinoye IO, Arslan H, dkk. Radiation shielding performance of a newly synthesized bismuth borate glass system. Radiat Phys Chem. Maret 2023; 204:110711.
  9. Şengül A. Gamma-ray attenuation properties of polymer biomaterials: Experiment, XCOM and GAMOS results. J Radiat Res Appl Sci. Desember 2023;16(4):100702.
  10. Şakar E, Özpolat ÖF, Alım B, Sayyed MI, Kurudirek M. Phy-X / PSD: Development of a user-friendly online software for calculation of parameters relevant to radiation shielding and dosimetry. Radiat Phys Chem. Januari 2020; 166:108496.
  11. Alver Ü, Duran SU, Demirköz MB, Muçoğllava B, Aslan M, Çava K, dkk. Ulexite/HDPE-Bi<sub>2</sub>O<sub>3</sub>/HDPE layered composites for neutron and gamma radiation shielding. Appl Radiat Isot. Oktober 2023; 200:110940.
  12. Alomayrah N, Albarqi MM, Alsulami RA, Alrowaili ZA, Eke C, Kebaili I, dkk. Effect of CaF<sub>2</sub> on the radiation attenuation properties of SiO<sub>2</sub>-P<sub>2</sub>O<sub>5</sub>-CaO-Na<sub>2</sub>O bioactive glasses: Theoretical and simulation studies. Results Phys. Maret 2024; 58:107441.
  13. Abdalsalam AH, Şakar E, Kaky KM, Mhareb MHA, Ceviz Şakar B, Sayyed MI, dkk. Investigation of gamma ray attenuation features of bismuth oxide nano powder reinforced high-density polyethylene matrix composites. Radiat Phys Chem. Maret 2020; 168:108537.
  14. Abouhaswa AS, Mhareb MHA, Alalawi A, Al-Buriah MS. Physical, structural, optical, and radiation shielding properties of B<sub>2</sub>O<sub>3</sub>-20Bi<sub>2</sub>O<sub>3</sub>-20Na<sub>2</sub>O-2Sb<sub>2</sub>O<sub>3</sub> glasses: Role of Sb<sub>2</sub>O<sub>3</sub>. J Non-Cryst Solids. September 2020; 543:120130.
  15. Intom S, Kalkornsurapranee E, Johns J, Kaewjaeng S, Kothan S, Hongtong W, dkk. Mechanical and radiation shielding properties of flexible material based on natural rubber/ Bi<sub>2</sub>O<sub>3</sub> composites. Radiat Phys Chem. Juli 2020; 172:108772.
  16. Alsaif NAM, Alotiby M, Hanfi MY, Mahmoud KA, Al-Yousef HA, Alotaibi BM, dkk. Comprehensive study of radiation shielding and mechanical features of Bi<sub>2</sub>O<sub>3</sub>-TeO<sub>2</sub>-B<sub>2</sub>O<sub>3</sub>-GeO<sub>2</sub> glasses. J Aust Ceram Soc. September 2021;57(4):1267-74.
  17. Yin S, Wang H, Wang S, Zhang J, Zhu Y. Effect of B<sub>2</sub>O<sub>3</sub> on the Radiation Shielding Performance of Telluride Lead Glass System. Crystals. 26 Januari 2022;12(2):178.
  18. Kaur P, Singh D, Singh T. Heavy metal oxide glasses as gamma rays shielding material. Nucl Eng Des. Oktober 2016; 307:364-76.
  19. Fathy IN, El-Sayed AA, Elfakharany ME, Mahmoud AA, Abouelnour MA, Mahmoud AS, dkk. Enhancing mechanical properties and radiation shielding of high-strength concrete with bulk lead oxide and granodiorite. Nucl Eng Des. December 2024; 429:113626.
  20. Hegazy HH, Al-Buriah MS, Alresheedi F, El-Agawany FI, Sriwunkum C, Neffati R, dkk. Nuclear shielding properties of B<sub>2</sub>O<sub>3</sub>-Bi<sub>2</sub>O<sub>3</sub>-SrO glasses modified with Nd<sub>2</sub>O<sub>3</sub>: Theoretical and simulation studies. Ceram Int. Januari 2021;47(2):2772-80.
  21. Singh KJ, Singh N, Kaundal RS, Singh K. Gamma-ray shielding and structural properties of PbO-SiO<sub>2</sub> glasses. Nucl Instrum Methods Phys Res Sect B Beam Interact Mater At. Maret 2008;266(6):944-8.

How to cite this article: Oki Ade Putra, Suci Faniandari, Dhani Nur Indra Syamputra, Muhammad Fahmi, Erik Bhukti Yutomo. Effect of ZrO<sub>2</sub> on radiation shielding properties of xZrO<sub>2</sub>-(55-x) B<sub>2</sub>O<sub>3</sub>-15Bi<sub>2</sub>O<sub>3</sub>-10MgO-20PbO Glass: XCOM and Phy-X/PSD database software. *International Journal of Research and Review*. 2024; 11(11): 79-88. DOI: <https://doi.org/10.52403/ijrr.20241110>

\*\*\*\*\*